

1 **Explosive activity of the last 1000 years at La Soufrière, St Vincent, Lesser Antilles**

2 Cole, P.D.^{1,*}, Robertson, R.A.E², Fedele, L.³, Scarpati, C.³

3 1 School of Geography, Earth and Environmental Sciences, Plymouth University, Drake Circus,
4 Plymouth (UK)

5 2 UWI Seismic Research Centre, University of the West Indies, St Augustine (Trinidad and Tobago)

6 3 Dipartimento di Scienze della Terra, dell'Ambiente e delle Risorse (DiSTAR), Università degli Studi
7 di Napoli Federico II - Via Cupa Nuova Cintia 21, 80126 Napoli (Italy)

8 * corresponding author (paul.cole@plymouth.ac.uk)

9

10 **Abstract**

11 The products of explosive activity of La Soufrière volcano on the island of St Vincent over the last
12 1000 years are described. Dates for the different eruptions were determined using information from
13 contemporary accounts, fieldwork and radiocarbon dating. Scoria-flow type pyroclastic density
14 currents (PDCs) dominate the products of both the historical eruptions (1979, 1902-03, 1812 CE) and
15 prehistoric eruptions (~1580 and 1440 CE) with subordinate fallout components associated with
16 several eruptions. Radiocarbon dating shows that these six eruptions define a crude cyclicity with
17 repose periods ranging between 77 and ~140 years and systematically decreasing in more recent
18 times.

19 Two prehistoric eruptions, in ~1440 and 1580 CE respectively, both produced magmatic lapilli fallout
20 and PDCs, and were fed by slightly more evolved magmas than the historical eruptions. The
21 eruptions in 1902 and 1812 CE had ash-rich, possible phreatomagmatic activity at their onset.

22 The iconic 1902-03 CE eruption generated radial distributed PDCs, which were responsible for the
23 deaths of ~1500 people. However, only small remnants of these deposits remain and the original
24 distribution cannot be determined from the preserved geology, which has important implications for
25 hazard studies.

26 Petrochemical work has shown that magmas involved in the explosive eruptions were quite narrow
27 in compositional range, mainly comprising basaltic andesites. The 1902-03 eruption involved a late
28 stage basaltic component in March 1903. However, activity in the last 1000 years generated notably
29 more homogeneous magmas with a narrower range than the older eruptive periods previously

30 reported in the literature, suggesting a significant variation in the magmatic reservoir feeding system
31 with time.

32 Keywords: La Soufrière, St Vincent; Pyroclastic Density Currents; 1902 eruption; radiocarbon dating;
33 Volcanic history;

34

35 **1. Introduction**

36 La Soufrière volcano on the island of St Vincent is the most active subaerial volcano in Eastern
37 Caribbean. It last erupted in 1979, an explosive eruption that had a volcanic explosivity index (VEI) of
38 3 which necessitated the evacuation of 20,000 people from around the volcano. Prior to this, there
39 have been three other historical explosive eruptions in 1718, 1812 and 1902/03. The 1902/03
40 eruption, of VEI 4 magnitude, which began on 7th May 1902, caused around 1500 fatalities but was
41 somewhat overlooked in the volcanological literature, possibly owing to its occurrence the day
42 before the catastrophic destruction of St. Pierre by Mt. Pelée in Martinique.

43 The four historical explosive eruptions define a weak cyclicity of explosive events occurring
44 approximately every 77 to 94 years. Knowledge of the Prehistoric activity (prior to 1700 in the
45 Caribbean Islands) of the volcano is limited (Robertson 2005). It is not known if this cyclicity in
46 explosive activity is a longer-lived feature of the volcano or if it is only represented by the historical
47 activity.

48 Many other volcanic systems show cycles of eruptive activity, occurring over regular time scales (e.g.
49 Luhr and Carmichael 1990; Odbert and Wadge 2014; Lamb et al 2014). Volcan de Colima (Mexico),
50 for example, has had at least 4 cycles, each of which has lasted around 100 years and appear to have
51 been terminated with a powerful Plinian explosive eruption (Luhr and Carmichael 1990). Such
52 cyclicity can provide important information regarding the behaviour of the volcanic system and
53 defining patterns of activity is important in forecasting of potential future volcanic activity.

54

55 Forecasting becomes more difficult for volcanoes with a limited historical record (Sparks and
56 Aspinall, 2004). Understanding the recent history of the activity of volcanoes is thus critical to
57 assessing the volcanic hazard for the surrounding region, and this is particularly true for La Soufrière,
58 St Vincent in what has historically been such an active volcano.

59

60 This paper addresses the gap in knowledge of the stratigraphy and petrology of the products of La
61 Soufrière's recent history, focussing on the last 1000 years. We describe the physical volcanology of

62 the products formed both by the historical and recent prehistoric explosive eruptions. We use
63 radiocarbon dating and stratigraphic studies to document these eruptions. In addition, we describe
64 the petrology and establish the geochemistry of these products.

65

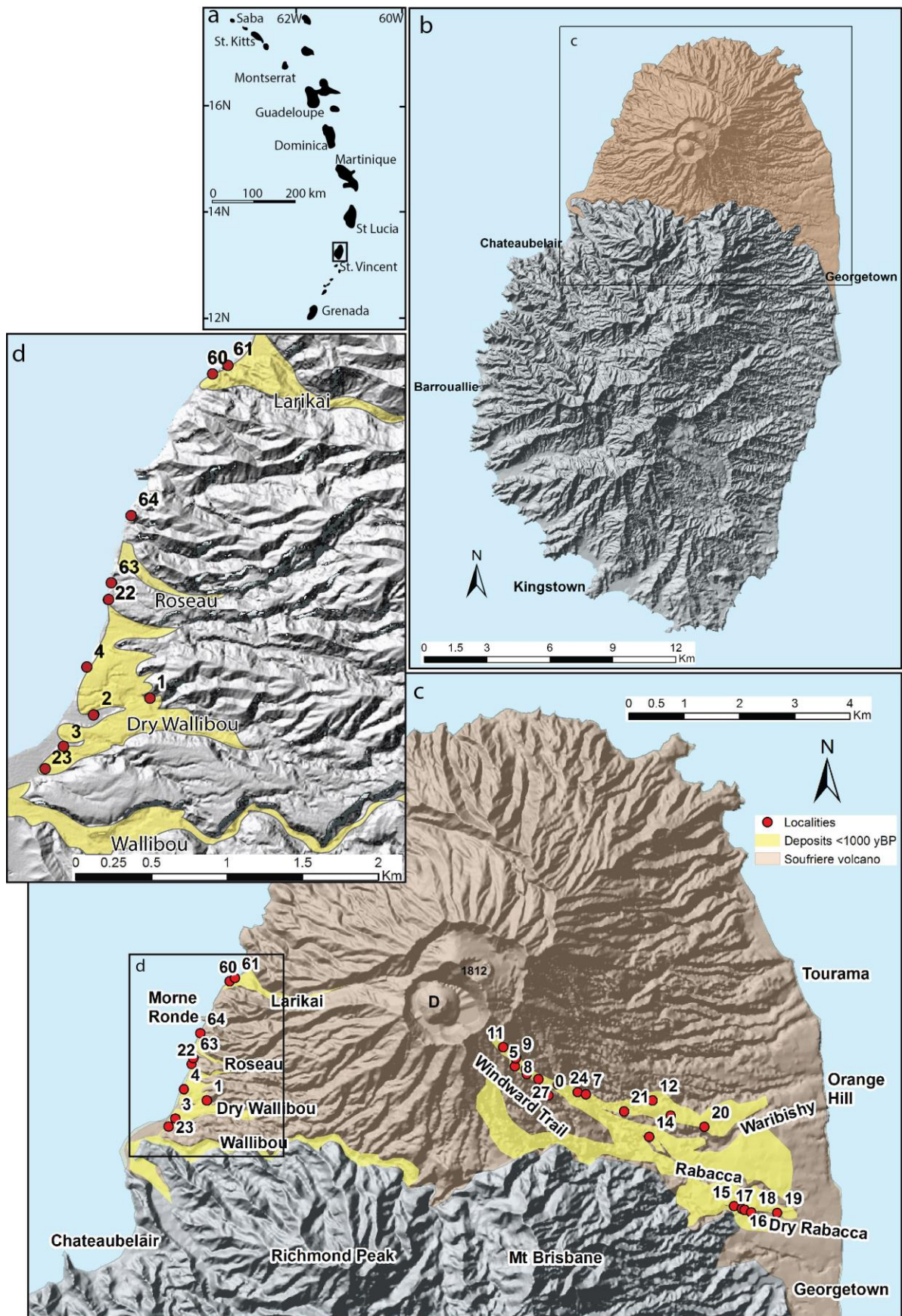
66

67 **2. Geological setting**

68 The island of St Vincent lies in the southern part of the Lesser Antilles (Fig. 1a), a 750 km-long
69 intraoceanic volcanic arc developed as the result of the relatively slow (i.e., ~2-4 cm/yr; Pindell et al.
70 1988; DeMets et al. 2000) subduction of the Atlantic/N-American plate beneath the Caribbean plate
71 (e.g., Macdonald et al. 2000). The island is 29 km from north to south and a maximum of 17 km from
72 east to west (Fig. 1b) and is composed of a series of dissected volcanic centres that young from
73 south to north, the youngest being the La Soufrière active stratovolcano. The oldest dated rocks on
74 the island are 2.74 Ma and La Soufrière's activity began in the late Pleistocene around 0.69 Ma
75 (Briden et al. 1979).

76 La Soufrière Volcano rises to a height of 1204 m (Fig.1b) and has a maximum basal diameter of 12
77 km from east to west. The shorter north to south diameter of 8.5 km is at least partly caused by the
78 southern flank abutting the steep northern part of the dissected older edifice of Richmond Peak and
79 Mt Brisbane (Fig.1c).

80 The summit complex of La Soufrière comprises an older Somma rim, forming the northern remnants
81 of a 2.2 km wide caldera-type structure open to the southwest (Le Friant et al. 2009; Fournier et al.,
82 2011). The present-day crater is nested within this caldera and is 1.5 km wide at its rim. It has a
83 maximum depth of 370 m on its northern side and a minimum of 100 m on its western edge. A lava
84 dome ('D' on Fig.1c) occupies the floor of the crater, is 850 m in diameter and 120 m high. It formed
85 at the end of the 1979 eruption and continued extruding until 1980. A small, 500 m wide crater,
86 formed in 1812, lies immediately northeast of, and cuts, the present-day crater ('1812' on Fig.1c).



88 **Fig.1** a) Location of St Vincent in the Eastern Caribbean. b) The island of St Vincent with La Soufrière
89 volcano shown in brown shading. c) Detail of La Soufrière volcano. Numbered localities (red dots)
90 refer to measured sections, some of which are shown in Fig.3. Key valleys and localities mentioned
91 in the text are also shown. D = 1979-80 lava dome. 1812 = crater formed in 1812 eruption. d) Detail
92 of PDC deposits fans formed on the southwest coast, mostly accumulated by PDCs <1000 yr BP.

93

94 Knowledge of the prehistoric activity of La Soufrière is scant. The lowermost flanks are composed of
95 basaltic lavas, considered part of the prehistoric Somma volcano and are dated between 0.36 and
96 0.69 Ma (Briden et al., 1979). A Yellow pumiceous tephra (Yellow Tuff Formation) containing several
97 topography-mantling lapilli fallout layers, that can be traced across the northern part of the island
98 (Rowley 1978b), overlie these lavas. Overlying this Yellow Tuff Formation on the lower flanks of La
99 Soufrière, are alluvial deposits and lahars interbedded with the deposits of primary pyroclastic
100 density currents (PDCs) (Robertson 2005). St. Vincent has also had effusive eruptions; such as in
101 1971, when a lava dome was erupted over a period of 4 months (Aspinall et al. 1973; Shepherd et al.
102 1979; Graham and Thirlwall 1981).

103

104

105 **3. Contemporary accounts of the historical explosive eruptions**

106 **3.1 1718 CE**

107 There is little geological or volcanological information related to the 1718 eruption from
108 contemporary documents. Dafoe (1718) describes tephra fallout up to approximately 30 cm in
109 thickness which occurred on ships in the region and also on several other Caribbean islands,
110 including Martinique (up to approx. 20 cm of tephra) as well as on Barbados, St Kitts, and possibly
111 the Dominican Republic (Anderson and Flett, 1903). Solely the native Caribs populated the island at
112 this time. There is however no information relating to the products on the island or any evidence of
113 resulting fatalities, although (Dafoe 1718) states that incandescence was observed from ships. Thus
114 the evidence indicates there was a not inconsiderable explosive eruption at this time.

115 A steaming dome was present in the crater in 1784 (Anderson and Yonge 1785) which has been used
116 to speculate on the possibly effusive eruption at this time.

117

118 **3.2 1812 CE**

119 The eruption began at midday on 27th April, after a series of more than 200 earthquakes were
120 reported over the previous year (various contemporary newspapers). Semi-continuous tephra fallout
121 occurred for three days until 30th April when, associated with apparently continuous tremor, the
122 eruption intensified. The following account of part of the eruption is of note (Blue Book 1902) ‘...and
123 *scaling every obstacle, carrying rocks and woods together in its course down the slope of the*
124 *mountain, until it precipitated itself down some vast ravine, concealed from our sight by the*
125 *intervening ridges of Morne Ronde. Vast globular bodies of fire were seen projected from the fiery*
126 *furnace, and bursting, fell back into it, or over it on the surrounding bushes, which were instantly set*
127 *in flames. About four hours from the lava boiling over the crater it reached the sea, as we could*
128 *observe from the reflection of the fire and the electric flashes attending it. About half-past one*
129 *another stream of lava was seen descending to the eastward towards Rabaka.’ Furthermore, as a*

130 number of these accounts (e.g. Shepherd, 1831) refer to ‘lava emissions’ it seems likely that these
131 phenomena involved hot material. While these could be lahars, the death of 50 people, as well as
132 extensive cattle and human fatalities in the Wallibou region to the southwest, indicate that these
133 were PDCs (Shepherd, 1831; Smith, 2011).

134 Tephra fallout associated with the 1812 eruption continued for several days significantly affecting
135 the eastern side of the island (Carib territory). Reports (Shepherd 1831) indicate 10 -20cm of tephra
136 fallout in several regions on the eastern flanks of the volcano. Ashfall also occurred for 18 hours in
137 Barbados (Smith 2011).

138

139

140 **3.3 1902-03 CE**

141 The 1902-03 eruption was extraordinarily well-documented in a series of contemporary accounts
142 including the detailed documents of Tempest Anderson and co-workers (e.g. Anderson and Flett
143 1903, Hovey 1903, Anderson 1908). These documents provide a rich record of the products of this
144 eruption and its impact on the island. There were three main phases: the first on 6th May, another in
145 September and October 1902 and the final phase in March 1903. The eruption began on 6th May
146 1902 after around 13 months of precursory felt seismicity. A crater lake existed prior to the eruption
147 and initial activity comprised a series of explosions with considerable steam involvement. The first
148 observations of incandescence at the crater were made during the evening of 6th May. Estimates
149 from contemporary sources indicate that eruption columns, associated with some of the initial
150 precursory explosions, reached > 1 km above the crater rim.

151 Tephra fallout started around 11 am on the morning of 7th May with fine ash fall, and an increase in
152 the calibre of fallout was reported, with lapilli sized fallout being reported on the south eastern side
153 of the volcano, in the Orange hill region, at around 12 pm.

154 At around 2pm on 7th May the paroxysmal phase of the eruption occurred with the formation of
155 what was initially termed the 'great black cloud' by Anderson and Flett (1903). These descriptions
156 relate to the formation of an extensive PDC, which travelled down nearly all flanks of the volcano,
157 resulting in more than 1500 fatalities (Pyle et al., 2018). This PDC reached the coastline in a number
158 of places and continued across the sea for several kilometres.

159 Further significant explosive activity occurred between 13 and 14 October 1902, and 21 and 30
160 March 1903 (Anderson 1908). Activity both in October 1902 and in March 1903 accumulated
161 deposits confined at base of the Larikai valley (Anderson 1908 p290 and 295) which are likely to have
162 been formed by PDCs. Extensive tephra fallout occurred associated with both events, in October
163 1902 up to 20 cm of scoria fallout was reported on the coast to the east of the volcano. Black,
164 vesicular lapilli deposit, up to 12.5 cm thick, were observed in Tourama, on the eastern flank, in
165 March 1903. Significant tephra fallout also occurred in Barbados associated with both these events
166 (Anderson 1908).

167

168 **3.4 1979**

169 The 1979 eruption began suddenly on the 13 April following elevated seismicity. The explosive
170 phase, consisting of a series of 11 Vulcanian type explosions, occurred over 13 days until 26th April.
171 Eruption columns developed from a number of these explosions reached 18 km above sea level
172 (Brazier et al 1982). The explosion on 17th April generated radial 'base surge type' PDCs to a distance
173 of 2 km from the crater (Shepherd and Sigurdsson 1982). Minor, completely valley confined, PDCs
174 descended the Larikai valley reaching the sea to the west, as well as the Roseau valley to the
175 southwest and part way down the Rabacca valley to the southeast (Shepherd et al. 1979). Ashfall
176 occurred extensively across the island and on the island of Barbados.

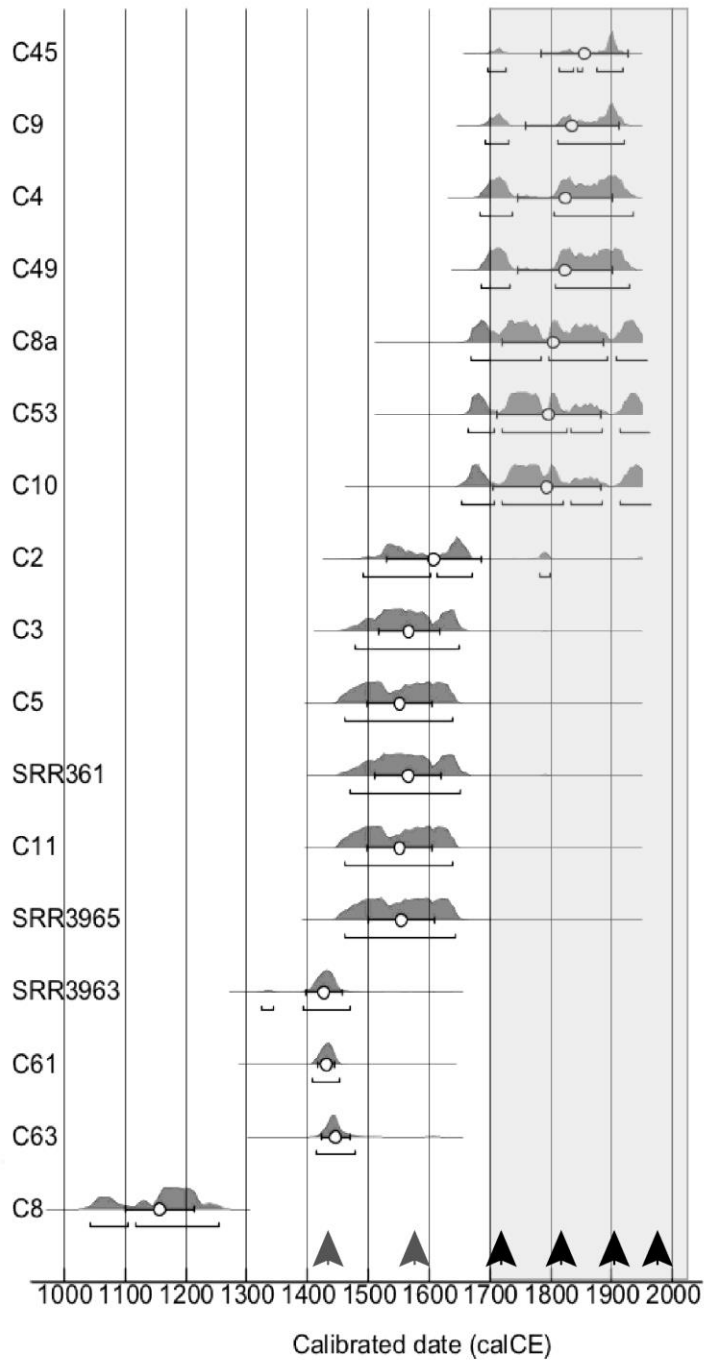
177

178 **4. Radiocarbon dating**

179 To relate the exposed products on the flanks of the volcano to specific eruptions, samples of
180 charcoal were collected and radiocarbon dated from a range of primary PDC deposits that represent
181 the youngest deposits formed in the volcano recent history.

182 Previously, Robertson (2005) listed eighty-one radiocarbon dates from this volcano, compiled from
183 three unpublished PhD and MPhil theses (Rowley 1978a, Robertson 1992 and Heath 1997), mostly
184 with limited stratigraphic information. These dates show distinct clusters, one comprising 53 dates
185 that range from ~ 600 yr BP to present day, whereas a second older cluster of 25 dates mainly from
186 the southeast and eastern flanks range from ~2000 to 5000 years. The radiocarbon dates of Hay
187 (1959) from the Rabacca valley at $3,800 \pm 300$ and $4,090 \pm 50$ yr BP correspond to this older range.

188 Our new radiocarbon dates are presented graphically in Figure 2 (with details in Table 1), and mostly
189 correspond to the earlier period, younger than 600 yr BP to present day. As all charcoal samples
190 except one were collected from primary pyroclastic deposits, we assume that these record the date
191 of the eruption that formed them. One sample (C8 Fig. 2 and Table 1) was a charcoal fragment
192 embedded in a palaeosol which is situated below the 1580 CE pyroclastic deposits on the Windward
193 Trail, approximately 1 km SE of the crater rim. Three pre-existing dates from Robertson (1992) were
194 also included in Fig.2 and Table 1 where, owing to stratigraphic information, we can be confident
195 that they relate to the deposits studied here.



196

197 **Fig 2** Calibrated radiocarbon dates used in this study. Plots are made using the Oxcal program
 198 version 4.3.2 (Bronk Ramsey 2009) using the IntCal13 Atmospheric curve. 95.4% confidence ranges
 199 are shown and median ages (open circles). The grey shaded zone relates to the historic period of St
 200 Vincent >1700 CE. Arrowheads show the timing of the six eruptions identified. For details of
 201 radiocarbon dates see Table 1

202

203

| Sample | Pre-treat | Conventional date (BP) | 95.4% (1 σ) Cal age range AD and relative area | Most probable Date CE | Stratigraphic unit |
|-----------|-------------------|------------------------|--|-----------------------|---|
| C45 | acid/alkali /acid | 20 ± 30 | 1696 – 1726 17% 1813 – 1837 12% 1844 – 1852 2% 1876 – 1919 65% | 1902*** | Uppermost PDC deposit of 3 PDCs in Dry Wallibou |
| C4 | | 79 ± 37 | 1682-1736 26.2% 1805-1935 69% | 1812, | Second deposit of 3 PDC deposits in Dry Wallibou |
| C49 | acid/alkali /acid | 90 ± 30 | 1685– 1733 26% 1796– 1928 69% | 1812, 1902 1718 | Uppermost thick (10m) unit on Wallibou coast |
| C8a | | 146 ± 35 | 1667-1783 45% 1725-1892 33% 1908 – pres 17% | 1718 1812 | Proximal SE flank Uppermost PDC deposit |
| C53 | acid/alkali /acid | 160± 30 | 1664 -1707 19% 1719- 1826 47% 1832 - 1884 13% 1914 – pres 19% | 1812 1718 | Windward trail SE flank 1 km from crater |
| C10 | | 172 ± 37 | 1654-1707 19% 1719-1820 48% 1832-1883 11% 1914-pres 19% | 1812 1718 | Proximal SE flank |
| C2 | | 273 ± 35 | 1491 – 1603 50% 1614- 1670 39% 1781-1799 6% | 1560 | Charcoal from thick PDC deposit midway up Dry Wallibou valley |
| C3 | | 313 ± 35 | 1477 – 1650 95.4% | 1566 | Third deposit of 3 PDC deposits in Dry Wallibou |
| SRR 3961* | | 315 ± 40 | 1471 – 1651 95.4% | 1553 | PDC deposits in Wallibou sea cliff |
| SRR 3965* | | 340 ± 40 | 1462-1642 95.4% | 1580 | Larikai sea cliff section midway up |
| C5 | | 347 ± 35 | 1460-1638 95.4% | 1590 | SW coast lowest PDC deposit fallout at base |
| C11 | | 347 ± 35 | 1460 -1638 95.4% | 1551 | Proximal SE flank, charcoal from coarse, fines free lapilli deposit |
| SRR 3963* | | 485 ± 40 | 1393 – 1470 95.4% | 1426 | Larikai sea cliff section lowermost unit. |
| C63 | acid/alkali/acid | 450 ± 30 | 1415 -1479 95.4% | 1445 | Larikai sea cliff section lowermost BAF deposit |
| C61 | acid/alkali/acid | 480 ± 30 | 1408-1452 95.4% | 1430 | Larikai sea cliff section Lowermost Scoria flow deposit |
| C8 | | 870 ± 37 | 1043-1104 22% 1118-1254 73% | 1157 | Large single charcoal fragment in soil on Windward Trail |

204

205 **Table 1** Radiocarbon dates - the three dates SRR361, 3965 and 3963 are from Robertson (1992).

206 Dates have been calibrated using the OXCAL version 4.3.2 program (Bronk Ramsey et al. 2009). All

207 samples were analysed by AMS (Accelerated mass Spectrometry.) Numbers in bold are the most
208 probable dates based on the calibration statistics.

209

210 Historical time, the date when Europeans colonised the Eastern Caribbean region, is from 1700 CE
211 onwards. As discussed earlier, there were four explosive eruptions in historical time while, prior to
212 this, there are no written accounts from the native Carib population that inhabited St Vincent.

213 The majority of radiocarbon dates fall into two broad groups, with little or no overlap between
214 them: a group relating to historical period (shaded grey on Fig.2), and a second group within
215 prehistoric time. The lack of overlap in the uncertainties between the historic and prehistoric groups
216 of dates indicates that the prehistoric ages represent distinct eruptions.

217 Radiocarbon dates from the period of the historical explosive eruptions: 1718, 1812 and 1902 are
218 associated with a large uncertainty related to carbon release from burning of fossil fuels since the
219 industrial revolution, therefore diluting radioactive carbon-14. As a consequence, the calibration of
220 dates <300 yr BP makes it difficult to determine which of the three major historical eruptions these
221 dates are associated with (Table 1 and Fig.2).

222 We further subdivided the prehistoric radiocarbon dates into two age groups: those occurring in the
223 16th Century (C2, C3, SRR3961, SRR3965, C5 and C11) and those in the mid-15th century (SRR3963,
224 C63 and C61). The 16th Century dates have uncertainties ranging from 1485 to the early 1640 CE
225 (Table 1 and Fig. 2). However, the 15th Century dates have narrower uncertainties ranging across
226 only 38 years from 1414 to 1452 CE (for 3 radiocarbon dates), with very little overlap in uncertainties
227 between the 15th and 16th Century group of dates (Fig. 2). Analysis shows that these two groups
228 statistically represent distinct dates (Stuiver et al 2018). Moreover, we used the 'Combine' function
229 of the OxCal v 4.3.2 program to determine model calibrated ages of the two groups, which give a
230 95.4% confidence limit of 1494 - 1632 CE for the 16th Century eruption and 1421 -1448 CE for the
231 15th century eruption.

232 To summarise this evidence strongly indicates that there were at least two prehistoric eruptions in
233 the last 600 years, one occurring in the mid-15th Century (mean age 1440 CE) and another occurring
234 in the later 16th Century (mean age 1580 CE).

235 The charcoal sample C8 with a calibrated age range between 1043 and 1254 yBP from a thick
236 palaeosol below the other eruptions described here indicates that there was a longer repose period
237 of at least 250 years and possibly much longer, prior to the 1440 yBP event.

238 Below we describe the products of the major historic eruptions, identified at least partly from
239 radiocarbon dating, and those related to the two prehistoric eruptions constrained at around 1580
240 CE and 1440 CE, respectively.

241

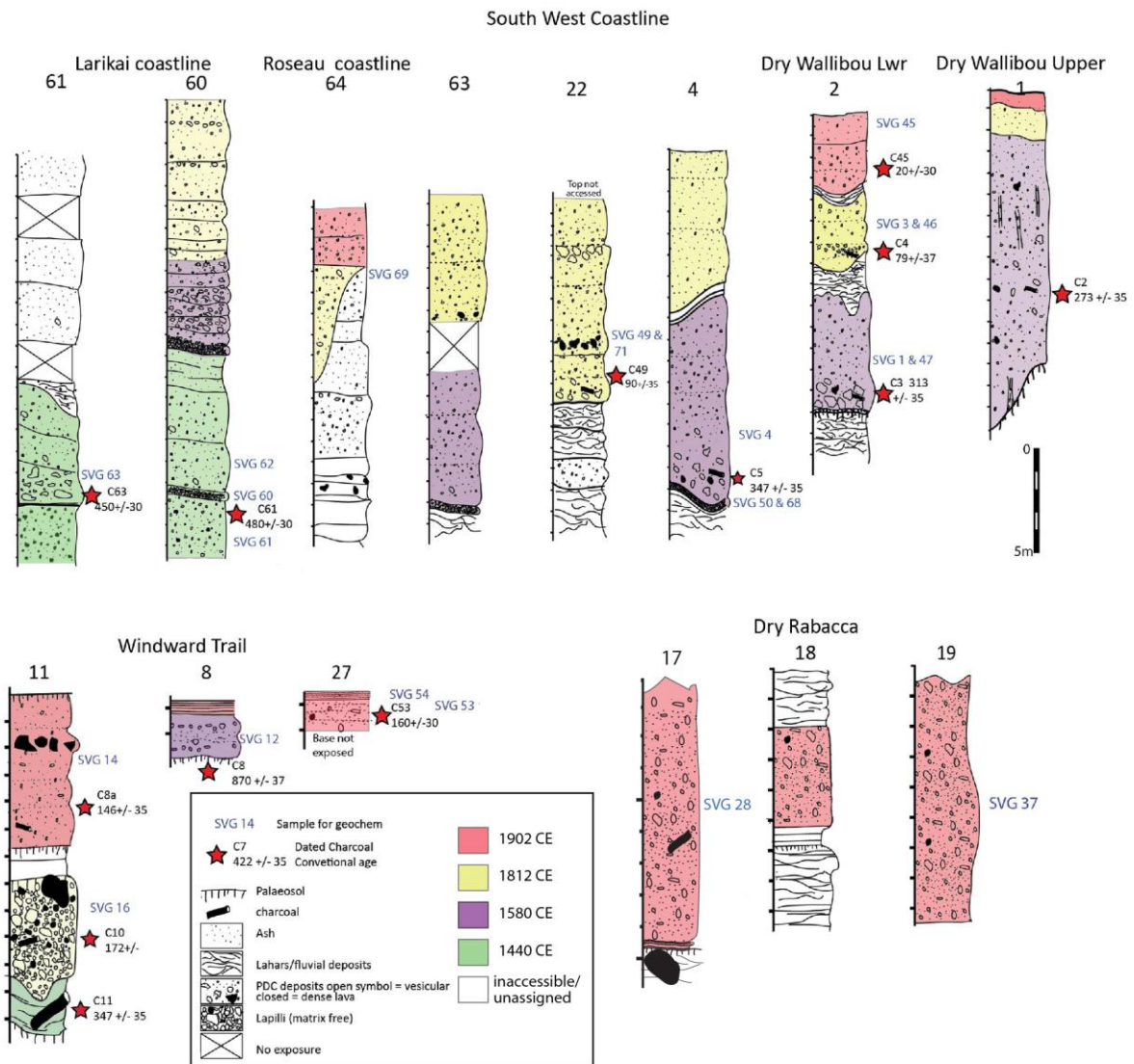
242

243 **5. Stratigraphy and products**

244 Measured sections at more than fifty localities on the south-western and south-eastern flanks were
245 documented during the course of this study (selected sections are shown in Figs. 1 and 3). These
246 exposures occur in and around drainages that extend from the southern part of the summit crater.

247 Valley confined PDCs associated with eruptions in the last 1000 years were strongly controlled by
248 the pre-existing crater and Somma rim, and apparently moved down the southern flanks.

249 Consequently, only the south-western and south-eastern flanks preserve a record of this activity
250 (Fig.1c). Even when PDCs spread radially around the volcano, as during the 1902 eruption, deposits
251 are not preserved in these regions, probably due to their thin and unconsolidated nature meaning
252 they were rapidly eroded.



253

254 **Fig 3** Selected measured sections from the flanks of the volcano. Blue letters refer to samples
 255 analysed for geochemistry. Red stars indicate charcoal samples for radiocarbon dating (only
 256 conventional dates are shown - for details see Table 1 and Fig.2). Numbers at top of sections refer to
 257 locations shown in Fig.1.

258 On the south-western side, valleys containing exposures of pyroclastic and volcanoclastic deposits
 259 include, from north to south, the Larikai (which drains the lowermost part of the crater rim), Roseau,
 260 Dry Wallibou and Wallibou river valleys, whereas on the south-eastern side the Rabacca and Dry
 261 Rabacca valleys drain directly from the crater (Fig.1c). Pyroclastic and volcanoclastic material erupted
 262 in the last 1000 years has formed a series of fans within and at the mouths of the valleys draining the
 263 southern part of the crater (Figs 1c and d).

264 La Soufrière's recent history is dominated by scoria-rich pyroclastic density currents, with
 265 subordinate deposits of both ash and lapilli fallout (Robertson 2005). Interbedded between the
 266 primary pyroclastic products, are water-reworked deposits such as lahars.

267 Deposits of the smaller 1979 explosive eruption have been nearly completely removed by erosion
268 and as a consequence the scattered remnants were not considered in this study.

269

270 **6. Volcanic products**

271 Each eruptive unit is described on the basis of its lithological and textural features. Grain-size and
272 component analyses of selected unconsolidated deposits were carried out in order to provide
273 further insight into the nature of the deposits. Although petrology and geochemistry are dealt with
274 later in a separate section, some simple geochemical trends (SiO_2) are described here to evaluate
275 possible compositional variations within eruptions. Interpretation of the eruptive and transport
276 mechanisms are suggested for each eruptive unit.

277

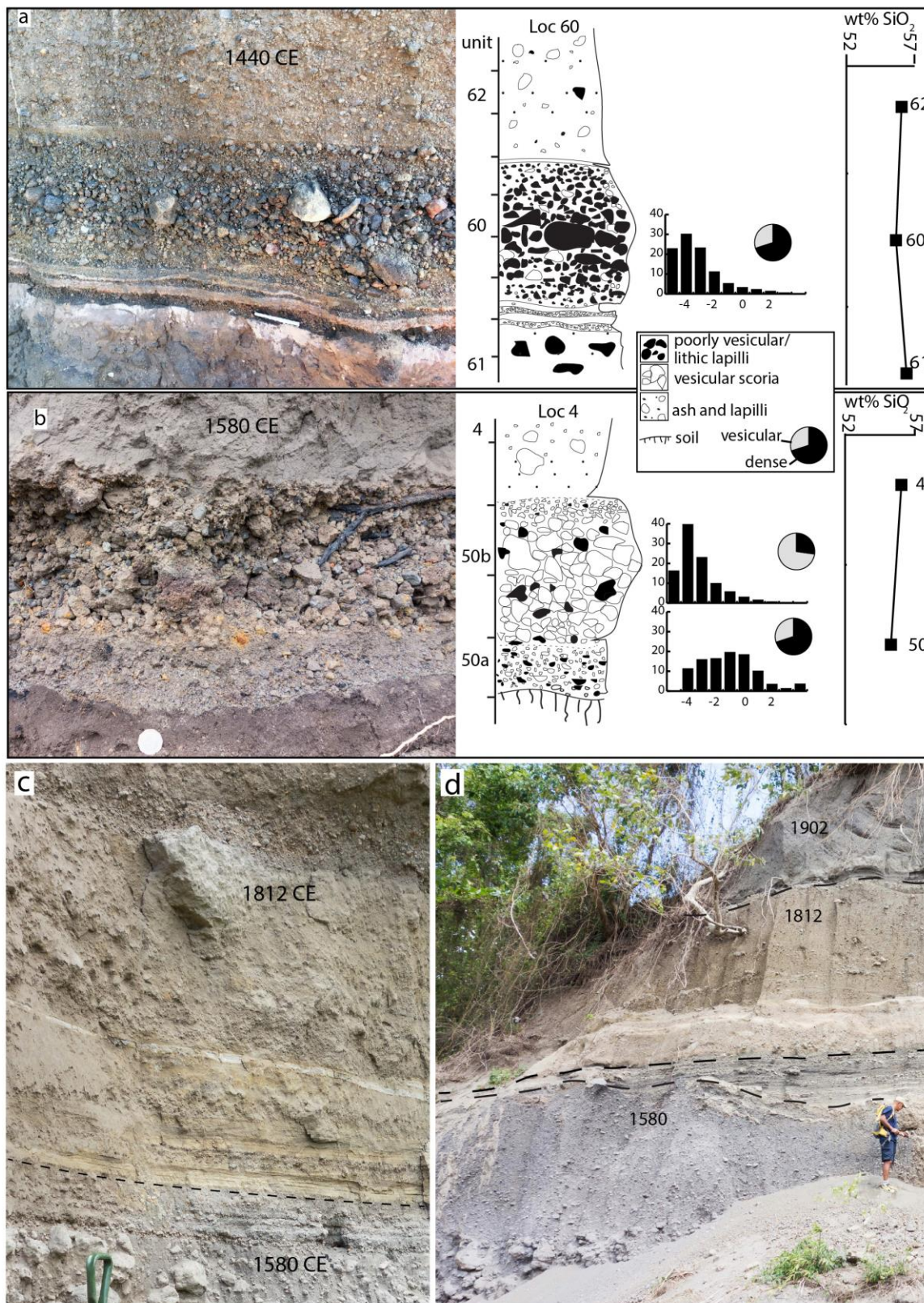
278 **6.1 1440 CE deposits**

279 These products were identified immediately south of the Larikai valley, which drains the lowest
280 point of the crater of La Soufrière, where a ~30 m thick sequence is exposed, representing a number
281 of eruptions (Fig.3 - section 60 and 61). Other exposures of this deposit occur in the upper part of
282 the 'Windward trail' on the south east flank (Fig.1).

283 At Larikai the lowermost part of the sequence is formed by > 4 m of massive, poorly-sorted deposit,
284 rich in dark grey to mauve feldspar-phyric scoria clasts that are notably poorly vesicular (unit 61, Fig
285 4a). These dense, scoria clasts are up to 35 cm across, although typical sizes are around 10 cm. The
286 scoria deposit is overlain by a coarse-grained, well-sorted lapilli layer that is up to 45 cm thick (Figs 3
287 section 60 and 61 and unit 60, Fig.4a). The lowermost part comprises thin cm scale, fine-grained
288 lapilli and interbedded ash layers (< 2 cm) showing notable lateral thickness variations. The main
289 part (uppermost 30 cm) of the lapilli displays reverse to normal grading, and is composed
290 predominantly of dense, poorly-vesicular juvenile clasts and abundant dense lava fragments.

291 Vesicular scoria form only 18 wt% of clasts > 2 mm (unit 60, Fig.4a). Erosively overlying this lapilli
292 several reverse graded, scoria-rich beds, up to 1.5 m thick, form a 5 m thick sequence (unit 61, Fig
293 4a). Each bed comprises poorly sorted, ash-rich deposit containing dark grey to black, plagioclase-
294 phyric vesicular scoria clasts up to 50 cm across. There are no significant variations in SiO_2 between

295 different parts of the same eruptive unit (Fig.4a).



296

297 **Fig 4 a)** Sequence associated with the 1440 CE eruption, immediately south of the Larikai valley (Loc
298 60 on Fig 1). At the base: poorly-sorted, scoria deposit; middle: lapilli fallout layer; top: reverse

299 graded, scoria-rich beds. Grainsize histograms and pie charts show components >2mm in size, grey=
300 vesicular scoria, black = dense lava. On the right is also shown the SiO₂ variation with stratigraphic
301 height. b) Lapilli fallout resting on the palaeosol at the base of the 1580 CE deposits(Loc 4 on Fig.1).
302 The lapilli deposit is overlain by a massive, poorly sorted, scoria-rich deposit. Grainsize histograms
303 are shown. Pie charts show components >2mm in size. On the right is also shown the SiO₂ variation
304 with stratigraphic height. c) Basal 2 m of 1812 CE deposits in the Dry Wallibou valley (near Loc 2 on
305 Figs. 1 and 3). Thin ash layers are interbedded with thin coarser, massive poorly sorted layers and
306 cross-bedded deposits. Deposits sit atop 1580 CE PDCs. d) Sequence of three PDC deposits exposed
307 in the northern wall of the Dry Wallibou valley on the southwest flank (Loc 2 on Figs.1 and 3). The
308 uppermost deposit is interpreted as 7th May 1902 PDC deposit, with 1812 CE and 1580 CE below.
309 Dashed lines enclose lahars and fluvial deposits interbedded between the primary eruptive units.

310

311 Owing to the presence of abundant poorly vesicular juvenile material, we interpret the lowermost
312 units of this sequence as 'block and ash flow type PDCs', possibly relating to lava dome collapses in
313 the crater. The lapilli layer is interpreted as fallout from a considerable eruption column and the
314 beds in the uppermost part are scoriaceous PDC deposits typical of St Vincent's recent activity,
315 derived from eruption column collapse.

316

317 **6.2 1580 CE deposits**

318 These products form some of the lowermost primary pyroclastic deposits around the Wallibou and
319 Dry Wallibou valleys and the coastal exposures between them (Fig.3 sections 1-4) and overlie
320 fluvial reworked volcanoclastic deposits. Up to 30 cm of distinctive well-sorted scoria lapilli form
321 the lowermost part (units 50 a and b, Fig.4b). This lapilli unit is composed of a lower finer grained, 8
322 cm thick part that is notably poor (30 wt% > 2 mm) in vesicular scoria (50a) and an upper, coarser,
323 normally graded, 22 cm thick unit containing abundant (72 wt% > 2 mm), highly-vesicular, pale grey
324 scoria clasts (unit 50b, Fig 4b). Subordinate dense lava and hydrothermally altered lithic clasts are
325 also present within this lapilli layer.

326 Massive, poorly sorted, scoria-rich deposits overlie the lapilli layer (unit 4, Fig 4b). These are locally >
327 30 m thick in the lower reaches of the Dry Wallibou valley on the SW flank, forming the thickest
328 deposits of this unit. More typically these massive deposits are ~5 m thick in continuous sections (>
329 100 m long) on the southwest coast (Fig. 3, sections 1-4). Although generally massive and
330 structureless, in some sections a number of subunits can be recognised ranging between 1 and 3m in
331 thickness, defined by distinct changes in grainsize. Abundant fragments of carbonised wood occur
332 within these deposits. Accumulations of abundant, coarse (up to 70 cm in diameter), dark grey to
333 black vesicular scoria clasts are locally present at the base of these massive deposits, forming
334 discontinuous normal grading (Fig. 4 d). The basal lapilli layer is composed of slightly less evolved

335 (55.5 wt.% SiO₂) scoria than the overlying scoria-rich deposits (56.3 wt.% SiO₂) of the same eruption
336 although the differences are probably not significant (Fig. 4b) as all the other major and trace
337 elements are remarkably homogeneous (see “Petrology of the scoria clasts” section).

338 The basal lapilli layer is considered the product of fallout from a convecting eruption column at the
339 start of the eruption with the progression from a finer scoria-poor part (unit 50a, Fig 4b) to higher
340 column that generated the coarse scoria-rich phase (50b, Fig 4b). This lapilli layer is not present at
341 the base of all localities (see sec 1 Fig.3), presumably owing to erosion either by the later PDCs or
342 between phases of the same eruption. The overlying massive, poorly sorted deposits are interpreted
343 as the products of PDCs. Such an interpretation is supported by the abundance of charcoal, local
344 accumulations of coarse scoria clasts and large thicknesses variations observed. These latter were
345 probably related to valley filling of the PDCs in the deep ravines that extend from the crater, such as
346 the Dry Wallibou valley.

347 **6.3 1718-1812 CE deposits**

348 The lack of almost any contemporary information on the 1718 eruptions, coupled with an absence of
349 distinctive field characteristics and large uncertainty in radiocarbon ages makes the distinction of the
350 products of the 1718 and 1812 eruptions difficult.

351 Nevertheless, contemporary accounts of the 1812 eruption (described earlier) clearly indicate that
352 PDCs moved down a number of valleys to the west, southwest and south-eastern flanks of the
353 volcano. In the southwest, along the Dry Wallibou valley (Fig. 3), pyroclastic deposits underlying the
354 1902 products and on top of 1580 CE deposits (Fig. 4d) are lighter in colour and contain paler,
355 pumiceous material. In addition, they are generally finer-grained than overlying and underlying
356 deposits, containing only rare scoria clasts > 10 cm in diameter.

357 The basal part of this sequence contains a number of thin, 1-2cm thick, ash layers (Fig.4c). Several
358 layers display cross-bedding and are interbedded with thin <15 cm massive, poorly sorted deposits.
359 The upper part of this pyroclastic sequence is composed of 3 - 6m thick, poorly sorted, massive,
360 valley ponding deposits.

361 The lowermost ash-rich layers are interpreted as having been formed by fallout. The fact that ash fall
362 out dominated the first three days of the 1812 eruption suggest that these deposits relate to this
363 event. A radiocarbon date of charcoal from these deposits indicates that there is a 69% probability
364 that the age range is between 1805 and 1935 CE. As 1902-03 deposits overly this unit, we therefore
365 consider these deposits to be products of the 1812 eruption.

366 We suggest that the cross-bedded and thin massive deposits may be the product of low
367 concentration PDC, whereas the more massive units formed from higher concentration currents.

368

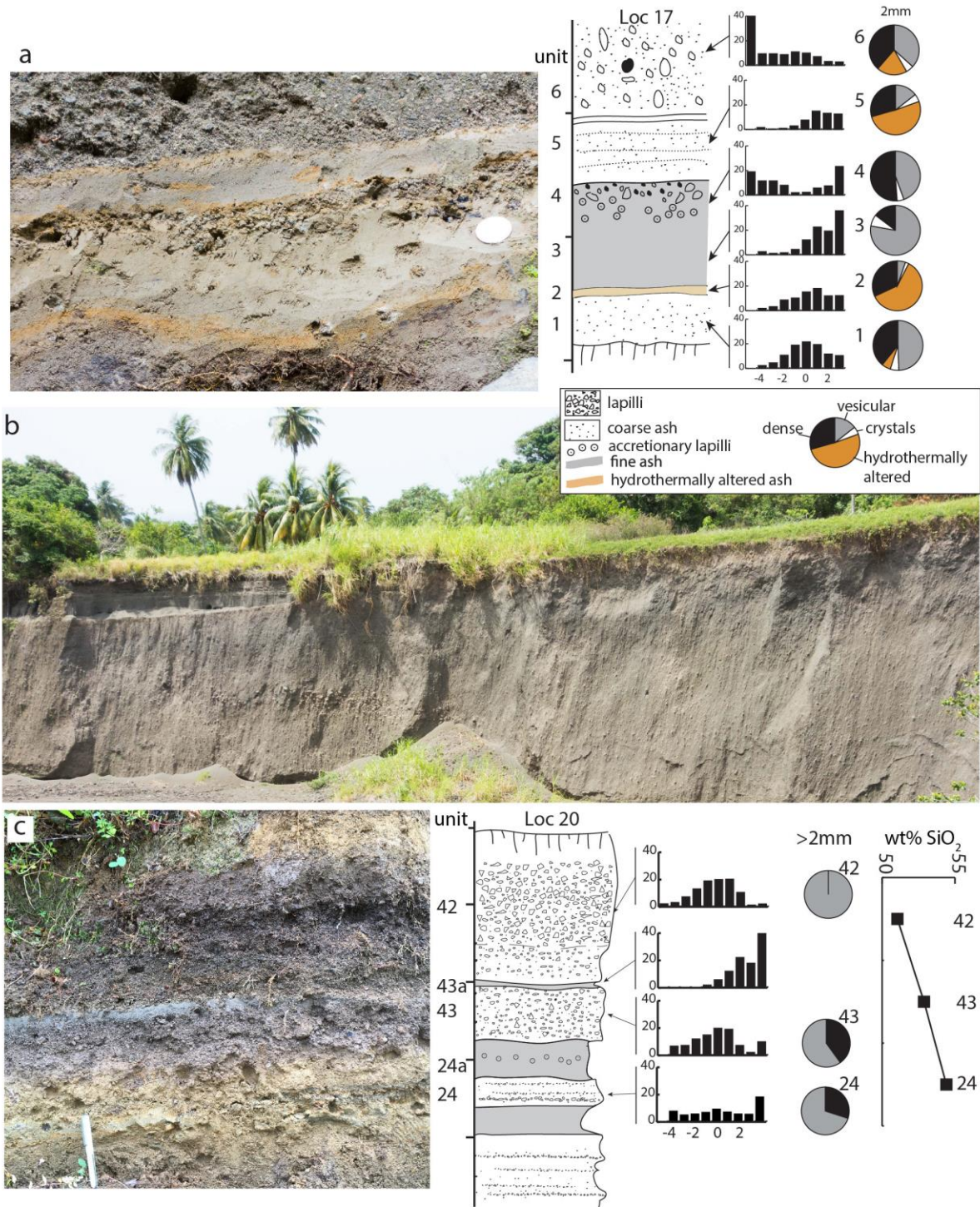
369 **6.3 1902-03 CE deposits**

370 Remnants of the products of the 1902-03 deposits are identifiable mainly on the southeast and
371 southwest flanks of the volcano (Fig. 3). In the Dry Rabacca valley to the southeast a basal tephra
372 sequence, up to 20 cm thick, overlies coarse-grained fluvial deposits (Fig. 3 section 18 and Fig. 5a).
373 The basal tephra sequence is composed of several mainly fine grained, ash-rich layers. A distinctive
374 2 cm thick, orange, fine lapilli layer occurs 2 cm above the base (unit 2, Fig 5a) , dominated by
375 abundant hydrothermally altered fragments. This is overlain by a 10 cm thick, ash-rich, accretionary
376 lapilli-bearing layer (unit 3, Fig 5a) that grades upwards into a coarser, diffuse vesicular scoria lapilli,
377 containing clasts up to 2 cm in diameter (unit4, Fig 5a). To the southwest the basal sequence is
378 either absent or locally present as 1 -2 cm of fine ash. Component analyses show that vesicular
379 juvenile scoria in varying quantities is a ubiquitous component throughout this sequence. Although
380 lithic material composed of both dense lavas and hydrothermally altered fragments form > 50% of
381 clasts (>2 mm) in a number of layers (Fig. 5a).

382 On the south-western side of the volcano, in the Dry Wallibou valley, the lowermost 1902 products
383 comprise up to 30 cm of dune bedded deposits that sit erosively on older (1718/1812 CE) pyroclastic
384 products (Fig. 4d). A massive, poorly sorted, indurated deposit, up to 28 cm thick, overlies this which
385 is in turn overlain by unconsolidated, massive, poorly sorted, scoria-rich deposits up to 5 m thick
386 (Fig. 3 Section 2).

387 On the south-eastern flank, sections through 1902-03 products (Dry Rabacca valley) comprise thick,
388 > 20 m, massive, coarse-grained, poorly sorted scoria-rich deposits (Figs. 3 and 5b) overlying the
389 basal tephra sequence. These deposits are structureless without stratification, although there is
390 some slight coarsening within the central part (Fig. 5b). On ridges and topographic highs on the
391 south-eastern flank in the region between Orange Hill and the Windward trail region (around 1 – 4
392 km from the crater) the uppermost 1902-03 deposits are formed by a distinctive sequence (Fig. 5c).
393 Poorly sorted, stratified deposits (unit 24, Fig 5c) up 60 cm thick, containing thin, discontinuous
394 lenses of fine lapilli, form the base of the sequence and rest on a weakly developed palaeosol (not
395 shown in Fig 5c). Locally a 5cm thick, fine grained, accretionary lapilli bearing ash layer caps this unit
396 (unit 24a, Fig 5c). A 12 cm thick grey, well-sorted lapilli layer overlies this (unit 43, Fig 5c) , although
397 outsized vesicular scoria blocks form ballistic impact structures, and is capped by up to 2 cm of fine

398 ash (unit 43a, Fig 5c). The uppermost unit is a distinctive dark, well-sorted lapilli layer, up to 40 cm
 399 in thickness, composed almost entirely of vesicular purple to black scoria lapilli (unit 42, Fig 5c).
 400 Dense (lithic) lava fragments are notably rare to absent from this layer. Geochemical analyses show
 401 that the lower stratified deposits contain basaltic andesite scoria with 54 wt.% SiO₂, whereas the
 402 uppermost lapilli fallout is basaltic in composition, 50-51 wt.% SiO₂ (Fig.5 c).



404 **Fig 5** a) Basal part of 7th May 1902 fallout sequence, exposed in the Dry Rabacca valley (near Loc 17
405 on Fig.1). b) Massive 7th May 1902 PDC deposits exposed in the Dry Rabacca valley (Loc 19 on Fig.1).
406 c) Stratified 7th May 1902 PDC deposits (orange), overlain by pinkish lapilli and a thin ash and dark
407 brown scoria-rich lapilli fallout layers thought to be formed by October 1902 and March 1903
408 activity, respectively. Photo of the described stratigraphic sequence (on the left) with representative
409 measured section (Loc 20 on Fig.1). Grainsize histograms and component pie charts depict
410 components >2 mm in size: grey = vesicular scoria, black = dense lava; orange = hydrothermally
411 altered lithic material. On the right is also shown the SiO₂ variation with stratigraphic height.

412 The basal tephra sequence in the Dry Rabacca valley is interpreted to have been formed by fallout
413 during the initial phase of activity in the late morning of 7th May 1902. Within this sequence the
414 coarser scoria lapilli horizon, within otherwise ash-rich material, is considered to represent fallout
415 from magmatic, Vulcanian style, explosions and possible correlates with an increase in calibre of
416 fallout described in contemporary documents that occurred at 12 pm on 7th May (Anderson and Flett
417 1903). The presence of vesicular scoria clasts throughout the sequence indicate widespread
418 fragmentation of gas-rich magma from the onset of eruptive activity. However, the abundance of
419 hydrothermally altered lithic clasts (which dominate some layers) and accretionary lapilli suggests
420 that phreatomagmatic activity generated some of these ash layers.

421 We interpret the massive deposits of the upper part of the sequence to have accumulated from high
422 concentration PDCs that were clearly valley confined and formed during the paroxysmal phase of the
423 eruption on the afternoon of 7 May 1902. Moreover, contemporary reports, from field studies, in
424 the weeks immediately after the eruption, described a 'glacier like' deposit within and blocking the
425 Rabacca valley (see Plate39 Fig.1 of Hovey 1903), that is now referred to as the Dry Rabacca valley.
426 Massive deposits exposed in walls of this valley are considered the dissected remnants of this
427 'glacier like' PDC deposit (Fig. 2 and 5 b).

428 In the Dry Wallibou, on the SW side, dune bedded deposits represent initial dilute PDCs with the
429 indurated massive deposit possibly representing a lahar formed contemporaneously with the initial
430 PDCs.

431 The thin, crudely stratified, poorly sorted deposits confined on the ridges are interpreted as products
432 of low particle concentration PDCs, related to the paroxysmal phase, on the afternoon of 7th May
433 1902 that swept radially away from the crater. The grey intermediate lapilli layer is interpreted to
434 represent fallout from October 1902 activity and the uppermost lithic-free, scoria lapilli fallout layer
435 was formed by explosive activity in March 1903. Such an interpretation is supported by the basaltic
436 composition of these lapilli as Roobol and Smith (1975) showed that the products of the March 1903
437 eruption were basaltic.

438

439

440 **7. Petrology of the scoria clasts**

441 Thirty single scoria samples belonging to the investigated La Soufrière eruptions were collected and
442 then processed for petrochemical characterization at the DiSTAR laboratories (Napoli, Italy). Samples
443 were crushed, washed in deionized water, dried out and pulverized in a low-blank agate mill. Rock
444 powders were analysed by ICP-OES (Inductively-Coupled Optical Emission Spectrometry) and ICP-MS
445 (Inductively-Coupled Plasma Mass Spectrometry) for major- and trace elements and weight loss on
446 ignition (LOI) at ActLabs (Ontario, Canada). Samples were mixed with a flux of lithium metaborate and
447 lithium tetraborate, and fused in an induction furnace. The melts were poured into a solution of 5%
448 nitric acid containing an internal standard and mixed continuously until completely dissolved (~30
449 minutes). The samples were analysed for major oxides and selected trace elements (Ba, Be, Sc, Sr, V,
450 Y and Zr) by Thermo Jarrell-Ash ENVIRO II or a Varian Vista 735 ICP optical spectrometer. Calibration
451 was performed using USGS and CANMET certified reference materials. Fused samples were diluted
452 and analysed by Perkin Elmer Sciex ELAN 6000, 6100 or 9000 ICP-MS for other trace elements. See
453 www.actlabs.com for full analytical details.

454 The composition of the main mineral and glass phases was analysed for a selection of 10
455 representative samples by EDS (energy dispersive spectrometry) at the DiSTAR (Napoli), using an
456 Oxford Instruments Microanalysis Unit equipped with an INCA X-act detector and a JEOL JSM-5310
457 microscope. Measurements were performed with an INCA X-stream pulse processor using a 15 kV
458 primary beam voltage, 50-100 μ A filament current, variable spot sizes and 50 seconds of acquisition
459 time. Relative analytical uncertainty is typically ~1-2% for major elements, ~3-5% for minor elements.
460 The results of all the petrological analyses are reported in the Electronic Supplementary Material 1.

461

462

463 **7.1 Petrography**

464 All juvenile scoria samples are strongly to moderately porphyritic (locally glomeroporphyritic) with
465 abundant plagioclase and clinopyroxene phenocrysts, together with less abundant olivine and/or
466 orthopyroxene, set in a weakly to moderately vesicular glassy groundmass. All the main crystal phases
467 typically contain inclusions of glass and other mineral phases (SMFig. 1). Numerous types of enclaves
468 (mostly holocrystalline, ranging from gabbroic to ultramafic) are also observed, a feature that is
469 extremely common for the juvenile products of the entire activity of the La Soufrière volcano (e.g.,
470 Heath et al. 1998; Tollan et al. 2012). Although generally similar, some small significant differences
471 occur between samples from different stratigraphic units (Table 2).

472 Scoria from the 1902-03 eruptions shows the widest petrographic variability with two different
 473 types present. The most common scoria type is dominated by large plagioclase phenocrysts (up to 2
 474 mm in length) with generally smaller colourless to pale green clinopyroxene, colourless to pale yellow
 475 orthopyroxene and few olivine phenocrysts/microphenocrysts (in decreasing order of abundance) and
 476 accessory opaque microphenocrysts (SMFig. 1a). In addition to occurring as well formed, euhedral
 477 pheno- and microphenocrysts both plagioclase and olivine occur occasionally as larger anhedral
 478 crystals (respectively 5-6 mm and ~1 mm). Glomerules of plagioclase, clinopyroxene and opaques
 479 (\pm olivine) are locally found.

480 A second type of 1902-03 scoria (e.g. SVG42, 44 and 72) shows a mafic-rich mineralogy characterized
 481 by plagioclase and clinopyroxene phenocrysts in similar quantities (~1 mm in length on average, with
 482 larger crystals up to ~2 mm) together with olivine, occasionally found as polymineralic aggregates
 483 (SMFig. 1c). Opaque oxides occur only as inclusions within clinopyroxene and olivine. The glassy
 484 groundmass displays local portions of high vesicularity with sparse microphenocrysts of plagioclase,
 485 clinopyroxene, olivine, orthopyroxene and opaque oxides set within a light brown glassy matrix,
 486 possibly suggesting mingling with some compositionally different magma batches.

487 The other eruptions described show a similar petrography - see Table 2 for details.

| sample | Eruption | Pl | Cpx | Opx | OI | Op | texture | notes |
|--------|-----------------------------------|------|-----|-----|----|----|--|--|
| SVG42 | 1902-03 (mafic-rich scoria) | XXX | XXX | | X | | strongly porphyritic, weakly vesicular; glassy groundmass | Cpx-rich enclave |
| SVG44 | | XXX | XXX | | X | | strongly porphyritic, moderately vesicular; glassy groundmass | light brown glass patches with higher vesicularity and crystals of Pl, Cpx, OI, Opx and Op; dunitic enclave |
| SVG72 | | XXX | XXX | | XX | | strongly porphyritic, moderately vesicular; glassy groundmass | OI+Cpx and micro-gabbroic enclaves |
| SVG24 | 1902-03 | XXX | XX | X | tr | tr | moderately porphyritic, (relatively) fine-grained, weakly vesicular; dusty groundmass | Amph+Pl+Cpx enclave |
| SVG28 | | XXXX | XX | X | tr | tr | strongly porphyritic, (relatively) fine-grained, moderately vesicular; glassy groundmass | |
| SVG14 | | XXXX | XX | x | x | x | strongly porphyritic + glomeroporphyritic, weakly vesicular; glassy groundmass | big green/brown Amph; common anhedral Pl |
| SVG3 | 1718-1812 | XXXX | XX | x | tr | x | strongly porphyritic, weakly vesicular; glassy groundmass | |
| SVG16 | | XXX | XX | x | tr | x | strongly porphyritic + glomeroporphyritic, moderately vesicular; glassy groundmass | troctolitic enclave |
| SVG1 | 1580 | XXXX | XX | x | tr | tr | strongly porphyritic + glomeroporphyritic, weakly vesicular; glassy groundmass | lava (Pl+Cpx) lithic; light brown glass patches with higher vesicularity |
| SVG4 | | XXXX | XX | X | tr | tr | strongly porphyritic + glomeroporphyritic, weakly vesicular; glassy groundmass | OI-gabbroic enclave |
| SVG50 | | XXXX | XX | x | | tr | strongly porphyritic + glomeroporphyritic, moderately vesicular; glassy groundmass | |

| | | | | | | | | |
|---|------|------|----|---|----|----|--|-----------------------|
| SVG60 | 1440 | XXX | XX | X | tr | tr | strongly porphyritic + glomeroporphyritic, moderately/weakly vesicular; dusty groundmass | micro-noritic enclave |
| SVG61 | | XXXX | XX | X | x | tr | strongly porphyritic + glomeroporphyritic, weakly vesicular; glassy groundmass | |
| SVG62 | | XXXX | XX | X | tr | tr | moderately porphyritic + glomeroporphyritic, moderately vesicular; dusty groundmass | |
| SVG63 | | XXXX | XX | x | x | tr | strongly porphyritic + glomeroporphyritic, moderately vesicular; dusty glassy groundmass | |
| XXXX = dominant, XXX = very common, XX = quite abundant, X = not very abundant, x = few crystals, tr = traces | | | | | | | | |

488

489

490 **Table 2** Summary of the main petrographic features of the collected scoria samples from the
 491 investigated historical and prehistorical eruptions of the La Soufrière volcano. Pl = plagioclase; Cpx =
 492 clinopyroxene; Opx = orthopyroxene; Ol = olivine; Op = opaque minerals; Amph = amphibole.

493

494

495

496

497 7.2 Mineral and glass chemistry

498 *Plagioclase*. Phenocrysts of plagioclase from all studied eruptions display a wide compositional range
 499 from labradorite/andesine to bytownite/anorthite (i.e. $An_{49-96}Ab_{5-50}Or_{0-2}$), with no systematic core to
 500 rim compositional differences, although single crystals commonly show a normal zoning. Occasional
 501 anhedral plagioclase from the 1902-03 scoria (SMFig. 1b) generally falls in the An-richer end of the
 502 above compositional spectrum (i.e. $An_{72-95}Ab_{4-28}Or_{0-1}$). Plagioclase inclusions in olivine, clinopyroxene,
 503 orthopyroxene are broadly homogeneous, possibly suggesting a contemporaneous segregation.

504

505 *Clinopyroxene*. A notably Ti-poor ($Ti < 0.051$ apfu) clinopyroxene is the main ferromagnesian phase of
 506 all the investigated samples, covering a wide range from (mainly aluminian, i.e., $Al > 0.1$ apfu;
 507 Morimoto, 1988) diopside to augite. In scoria from the historical eruptions, clinopyroxene is mostly
 508 augitic and covers the range $Wo_{35-45}En_{40-46}Fs_{13-20}$ [$Mg\# = Mg\# = \text{molar Mg}/(\text{Mg} + \text{Fe}^{2+}) = 0.69-0.78$]. A
 509 core to rim decrease of Mg# (from 0.71-0.77 to 0.70-0.72), coupled with Ca decrease (from 0.763-
 510 0.829 to 0.692-0.816 apfu), is evident only for 1718-1812 clinopyroxene. Less abundant diopsidic
 511 clinopyroxene is present mainly in the 1902-03 mafic-rich scoria crystal cores ($Wo_{45-51}En_{39-44}Fs_{8-13}$, $Mg\#$
 512 = 0.76-0.84).

513 Some anhedral clinopyroxene found in the 1902-03 mafic-rich scoria have remarkably Mg-rich
 514 aluminian diopsidic cores ($Wo_{46-50}En_{42-47}Fs_{6-9}$, $Al = 0.127-0.304$ apfu, $Mg\# = 0.83-0.88$) surrounded by
 515 Mg-poorer aluminium diopsidic/augitic rims ($Wo_{44-45}En_{41-43}Fs_{13-14}$, $Al = 0.132-0.195$ apfu, $Mg\# = 0.74-$
 516 0.78). Clinopyroxene from the prehistoric eruptions is generally more homogeneous (mostly augite,

517 with some sporadic diopside) and poorer in Mg (Mg# = 0.69-0.77) and Al (generally in the 0.060-0.126
518 apfu range, occasionally up to 0.220 apfu) with respect to that from the historical activity.

519

520 *Olivine*. A relatively abundant phenocryst phase only in the mafic-rich 1902-03 scoria samples,
521 characterized by a quite large compositional variation (Mg# = 0.71-0.86, with crystal cores being
522 generally Mg-richer). The fewer olivine phenocrysts/microphenocrysts analysed in the remaining
523 samples are generally more homogeneous and Mg-poorer, covering the Mg# range of 0.63-0.77.
524 Anhedronal olivine crystals from the historical eruptions display slightly Mg-richer compositions with
525 respect to phenocryst phases for both the 1902-03 (Mg# = 0.74-0.79 vs. 0.63-0.76) and the 1902/03
526 mafic-rich scoria (Mg# = 0.72-0.88, typically normally zoned). Within 1718-1812 scoria the large
527 anhedronal, occasionally rounded, olivine is significantly Mg-poorer, with Mg# = 0.65-0.76.

528

529 *Orthopyroxene*. A typical mineral phase in scoria in most eruptions, whereas it occurs only as
530 inclusions (Mg# = 0.65-0.71) within clinopyroxene phenocrysts in the 1902-03 mafic scoria.
531 Compositions are quite constant in all the analysed samples, with Mg concentrations being slightly
532 higher in the scoria from the 1902-03 (Mg# = 0.65-0.72) and 1718-1812 historical eruptions (Mg# =
533 0.64-0.70), with respect to those from the 1580 (Mg# = 0.63-0.67) and 1440 (Mg# = 0.63-0.68).

534

535 *Opaque minerals*. The main opaque mineral is Ti-magnetite, diffusely found as a
536 microphenocryst/microcryst in all but the 1902-03 mafic-rich samples. Compositions are basically
537 constant, mostly with Usp (ulvöspinel mol.%) and Mg# respectively in the ranges of ~30-40 mol.% and
538 0.09-0.12.

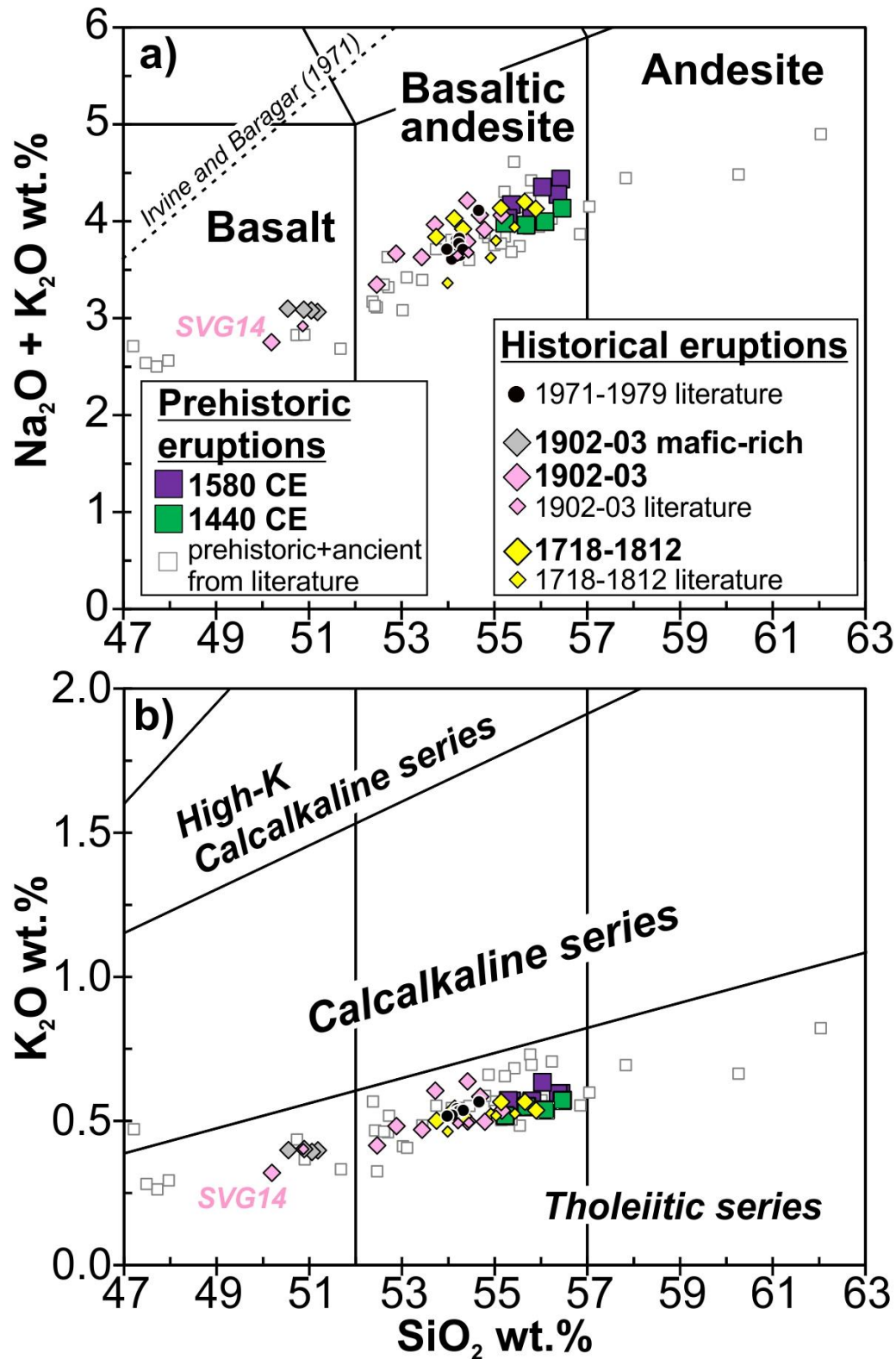
539

540 *Glass*. Analysed groundmass glass covers a notably wide compositional range. Although this might at
541 least in part reflect the variable crystallinity of the analysed samples, an overall increase in the degree
542 of evolution can be observed moving from basaltic andesite and andesite in the 1902-03 mafic-rich
543 scoria (SiO₂ = 56.6-62.6 wt.%; Mg# = 0.19-0.46), to dacite in the 1902-03 (SiO₂ = 64.4 wt.%, Mg# =
544 0.17), to andesite/dacite in the 1718-1812 (SiO₂ = 60.8-68.0 wt.%, Mg# = 0.21-0.34), dacite in the 1580
545 (SiO₂ = 64.4-65.9 wt.%, Mg# = 0.28-0.36) and 1440 samples (SiO₂ = 60.1-68.7 wt.%, Mg# = 0.12-0.27).
546 Glass inclusions in the main phenocryst phases, especially in plagioclase and clinopyroxene, basically
547 show similar chemical trends.

548

549 **7.4 Whole-rock geochemistry**

550 Scoria analysed show a relatively limited compositional range in terms of Total Alkalis vs. Silica
551 (TAS; Fig. 6a), ranging from basalts (mainly represented by 1902-03 mafic-rich scoria samples) to more
552 abundant basaltic andesites. Samples from the 1902-03 eruption show the greatest compositional
553 variability (i.e., SiO₂ = 50.2-54.8 wt.%), with the mafic-rich scoria at the least evolved end. Samples
554 from the 1718-1812 eruption also show some compositional variability, mainly overlapping with that
555 of the 1902-03 eruption but also including slightly more evolved compositions (SiO₂ = 53.7-55.9 wt.%).
556 Scoria from the prehistoric eruptions are generally notably homogeneous and more evolved (i.e., SiO₂
557 = 55.3-56.4 and 55.2-56.7 wt.%, respectively for 1580 and 1440).



558

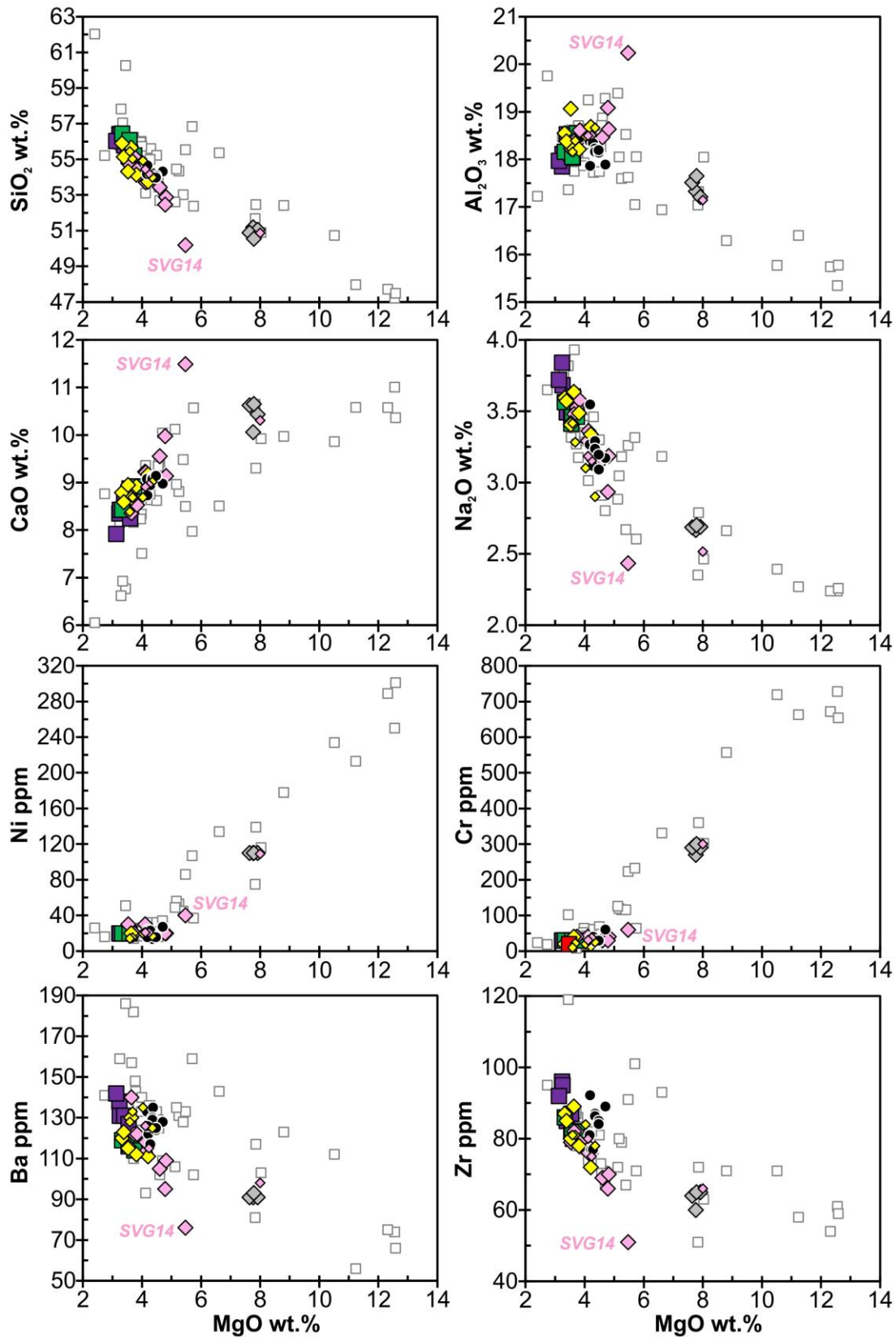
559 **Fig 6** a) TAS (Total Alkali vs. Silica; LeMaitre, 2002) and b) K_2O vs. SiO_2 (Le Maitre, 2002) diagrams for
 560 the analysed La Soufrière juvenile samples. Sample SVG14 (1902-03) showing some anomalous
 561 chemical features is highlighted (see text). Also shown are the literature data for the prehistoric and
 562 ancient activity (Heath et al., 1998) and 1971-79 eruptions (Graham and Thirlwall, 1981). In a) the
 563 dashed line separates the fields for subalkaline and alkaline rock series (Irvine and Baragar, 1971).
 564

565

566 Our samples fall well within the entire La Soufrière compositional field, which ranges from more
567 primitive basaltic (i.e., SiO₂ = 47.2-48.0 wt.%) to more evolved andesitic compositions (SiO₂ = 57.8-
568 62.3 wt.%) among the products of the prehistoric and ancient activity. Overall, the La Soufrière
569 samples depict a quite linear trend for a clearly subalkaline rock series with low-K tholeiitic affinity
570 (Fig. 6b). Although a detailed discussion on such topics is out of the scope of this paper, the serial
571 affinity of the products of the La Soufrière (as well as of those of the Lesser Antilles volcanism in
572 general) has been debated by a number of authors (e.g., Smith et al. 1996; Heath et al. 1998;
573 Macdonald et al. 2000 and references therein), and either tholeiitic, calcalkaline or transitional
574 affinities have been proposed. In any case, it is of note that our data is perfectly in line with published
575 data.

576 Harker-type binary variation diagrams (Fig. 7) depict quite linear differentiation trends, moving
577 from the 1902-03 mafic-rich scoria to the products of the prehistoric eruptions. With the only
578 exception of a single 1902-03 scoria sample (SVG14), a general decrease of MgO, CaO, Sc, Ni and Cr
579 and an increase of SiO₂, Na₂O, K₂O, Ba, Y, Zr seem to characterize the differentiation of the investigated
580 La Soufrière samples. In addition, both Al₂O₃ (first increasing and then decreasing) and Sc (first
581 remaining constant, then rapidly decreasing) experience an evident discontinuity in their
582 differentiation trends at SiO₂ ~52 wt.%. This is consistent with both petrography and mineral (and
583 glass) phases chemical variations, as well as with the overall literature for La Soufrière samples.

584



585

586 **Fig 7** Selected major- and trace element binary variation diagrams for the analysed La Soufrière
 587 juvenile samples. Sample SVG14 (1902-03) showing some anomalous chemical features is highlighted
 588 (see text). Symbols and literature data as in Fig. 7.

589

590 **8. Discussion**

591 ***8.1 Eruption Frequency and style***

592 Radiocarbon dating has allowed identification of two prehistoric eruptions that have occurred in the
593 last 1000 years at La Soufrière St Vincent. One in the 16th century with a mean calibrated age of 1580
594 CE (based on six dates), and another in the 15th Century with a mean calibrated age of 1440 CE
595 (three dates). Owing to the nature of the radiocarbon calibration curve together with a paucity of
596 distinctive features, it is difficult to separate the deposits of the 1718 and 1812 eruptions. Indeed, it
597 is possible that the eruption in 1718 generated limited PDCs and thus the studied deposits represent
598 mainly the 1812 eruption.

599 Our radiocarbon dating shows that over the last 1000 years there were at least six explosive
600 eruptions with a repose period varying between 77 and ~140 years, This gives a mean periodicity of
601 90 years between explosive eruptions from 1440 until 1979.

602 It is clear however that the repose period between eruptions has not remained constant with time.
603 A notable decrease in repose times is evident: > 300 yr before 1440 CE (although with large
604 uncertainty), 140 yr before 1580 CE, 138 yr before 1718, 96 yr before 1812, 90 yr before 1902-03
605 and 77 yr before 1979. This might indicate that a future eruption could be < 77 years since 1979,
606 giving rise to the possibility of an explosive eruption before 2059 if this trend were to continue,
607 although this is associated with a very large uncertainty and of course the volcano might not follow
608 the same pattern. The effusive activity which occurred in 1971 is not considered here, furthermore
609 there is the possibility of an effusive dome forming eruption around 1784 and others that may have
610 not been recorded. Including these effusive events would result in a different pattern of activity not
611 considered here.

612 Almost all the eruptions generated PDCs and in most cases numerous PDCs travelled down valleys
613 draining the southern and lowest part of the crater. Most of these PDCs deposits were scoria flows
614 (frequently referred to as 'Soufrière type', McBirney and Williams 1979) considered to have been
615 generated by collapse of eruption columns, as was originally proposed for the 1902 events by Hay
616 (1958). However evidence indicates that each eruption was quite different in terms of the
617 magnitude, initial ash-rich activity e.g. 1902, 1812 CE eruptions, or magmatic 'plinian type' lapilli
618 fallout 1580 CE. In addition PDC deposits at the base of the 1440 CE eruption do not contain
619 vesicular scoria and may have involved collapse of lava domes to generate block and ash flow types
620 PDCs, indeed lapilli fallout containing abundant dense, poorly vesicular clasts suggest powerful
621 Vulcanian explosions associated with destruction of such lava domes. Thus apart from Scoria-rich
622 'Soufrière type' PDCs which were involved with most eruptions, each event varied significantly.

623

624 The distribution of the products formed by eruptions in the last 1000 years indicates that the pre-
625 existing topography of the volcanic edifice has had a considerable effect on them. No products
626 formed in the last 1000 years crop out on the northern and eastern flanks. However, extensive
627 knowledge of the 1902 eruption demonstrates that dilute, low-concentration PDCs capable of
628 causing extensive fatalities travelled down the northern and eastern flanks. This highlights the
629 danger of using preserved geology in hazard analysis. Preservation of products from such activity is
630 extremely poor, particularly so on the steep flanks of a tropical volcano.

631 Most historical explosive activity was associated with abundant ashfall that extended to other
632 islands. Evidence indicates some of the initial 1902 activity was phreatomagmatic and the initial
633 1812 activity was also ash-rich. The presence of a crater lake prior to both these eruptions possibly
634 played an important role in this. The basal fallout sequence of the 1902-03 eruption also preserves
635 evidence of more intermittent explosive Vulcanian type activity. However, significant lapilli fallout
636 formed by considerable convecting eruption columns were only associated with the prehistoric
637 eruptions (1440 and 1580 CE).

638 The 1580 CE PDC deposits form a large part of the fans in and around the main valleys draining the
639 crater, in particular in the SW in coastal sections. These deposits form some of the thickest and most
640 widespread products of the last 1000 years, indicating that this eruption was potentially the largest
641 in the last 1000 years.

642

643 **8.2 Petrochemical implications**

644 The petrochemical characterization has revealed a relatively limited compositional variation of the
645 magmas feeding the most recent prehistoric and historical eruptions. Our new data are consistent
646 with the few available literature counterparts, and fall well within the wider compositional spectrum
647 defined by the dataset for the entire history of La Soufrière's activity. Chemical trends are quite
648 linear, suggesting a genetic relationship linking the most evolved products of the 1440 and 1580 CE
649 prehistoric eruptions with the progressively less evolved products of the 1718-1812 and 1902-03
650 historical eruptions. It could be proposed that the more evolved compositions of both the
651 prehistoric eruptions might have led to retention of volatiles and thus a more violent explosive
652 nature (consistent with the stratigraphic data for the 1580 CE eruption; see previous paragraph).

653 It seems likely that magma evolution was substantially driven by crystal fractionation firstly involving
654 mainly olivine, clinopyroxene and plagioclase (i.e., decreasing MgO, CaO, Ni, Cr, increasing Al₂O₃, and

655 alkalis) and then plagioclase, clinopyroxene, orthopyroxene and Fe-Ti oxides (decreasing Al_2O_3 ,
656 Fe_2O_3 tot and V at $\text{MgO} < 4$ wt.%). This is in line with the petrographic features of the two recognized
657 scoria types, as well as with the chemical trends of the analysed mineral and glass phases (see
658 “Petrography” and “Mineral and glass chemistry” sections).

659 Notably deviating is the composition of 1902-03 scoria sample SVG14, featuring the lowest SiO_2
660 coupled with unusually high Al_2O_3 (20.2 wt.%), CaO (11.5 wt.%) and Sr (232 ppm), and low MgO (5.47
661 wt.%), Sc (31 ppm), Ni (40 ppm) and Cr (60 ppm). Given the overall similarity in petrography and
662 mineral and glass chemistry of such sample with all the other 1902-03 scoria samples, and the
663 typical presence of notably An-rich anhedral plagioclase (up to An_{96} ; Fig. 6b), it seems likely that the
664 composition of this sample has been significantly modified by plagioclase cumulation. This testifies
665 to a limited additional role played by open-system processes (e.g., magma mixing, assimilation of
666 crystal mushes), which is plausible, given the common presence of cumulate-textured enclaves, in
667 the lava and pyroclasts of the La Soufrière volcano (e.g., Heath et al. 1998; Tollan et al. 2012), as well
668 the gabbroic to ultramafic enclaves reported for the investigated scoria samples (see “Petrography”
669 section and Table 2).

670 The paramount role of crystal fractionation in the evolution of La Soufrière magma has been long
671 recognised by both whole-rock and mineral petrochemical studies (Heath et al., 1998), and thorough
672 experimental work at various P and H_2O content conditions (Pichavant et al., 2002; Pichavant and
673 Macdonald, 2007; Melekhova et al., 2015). Although the existence of four (slightly) different magma
674 lineages related with differences in P (from 1.3 to < 0.4 GPa) and H_2O contents (2.3-4.5 wt.%) of the
675 parental magmas (plus occasional partial melting of water-poor high-MgO basalt that solidified at
676 depth; Melekhova et al., 2015) has been proposed, no attempt has been made to link these to a
677 specific periods of the volcanic history.

678 The possible existence of time-related trends in the composition of the magmas erupted at La
679 Soufrière can be thus only crudely evaluated through simple chemostratigraphic investigation. Older
680 sequences of the volcano ranging up to 600 ka (Figs. 6 and 7) show a much wider chemical variation
681 than the eruptions in the last 600 years reported here. In fact, the most recent products show the
682 narrowest range of composition in the volcano’s history. Further detailed study is required, possibly
683 allowing a better evaluation of the geochemical vertical trends within the deposits of a single
684 eruption (only occasionally and crudely evaluated here for stratigraphic sections showing the most
685 favourable exposure conditions; Figs. 4 and 5). However, what can be tentatively suggested at this
686 stage is that in the more recent history, magma might have more readily found the opportunity to
687 evolve and homogenise within shallow reservoirs eruption of relatively primitive basaltic magmas

688 occurred only rarely, as in the 1902-03 (possibly being evidence of magma chamber rejuvenation
689 acting as eruption trigger).

690

691 9. Conclusions

692 • The period of the last 600 years at La Soufrière St Vincent has involved six explosive
693 eruptions with repose periods of 77 and ~140 years. There is a decrease in the repose period
694 between explosive eruptions with time, with the shortest repose period between the most
695 recent explosive eruptions in 1902 and 1979

696

697 • Deposits formed are predominantly 'scoria flow type' PDCs formed by collapse of eruption
698 columns, although some block and ash flow type PDCs, associated with the collapse of lava
699 domes, were formed during the 1440 CE eruption

700

701 • Only the prehistoric eruptions in 1440 and 1580 CE, were associated significant lapilli fallout
702 deposits. These events were the most evolved geochemically with slightly higher SiO₂ values
703 than the historical events.

704

705 • Initial activity associated with the 1902-03 and 1812 eruption was ash-rich and, certainly for
706 1902, the products were rich in lithic material and accretionary lapilli. These features suggest
707 that the initial events of these eruptions were phreatomagmatic.

708

709 • Despite the paroxysmal PDCs formed on 7th May 1902 being spread largely radially around
710 the volcano, remnants of deposits are only preserved to the southwest and southeast,
711 highlighting the incomplete and unreliable nature of spatial extent, based on geologically
712 preserved products, for hazard analysis.

713

714 • Erupted basalt-basaltic andesite magmas are generally less variable in the last 600 years
715 with respect to the ancient phase of La Soufrière's activity. This possibly suggests that the
716 feeding magmatic system has attained the conditions for effective magma homogenisation
717 through fractional crystallisation (plus occasional open-system processes), only sporadically
718 allowing the emplacement of relatively primitive terms.

719

720

721 **Acknowledgements**

722 Lara Mani is thanked for assistance in the field, particularly on the initial visit to the Larikai. Jack
723 Palmer for help with initial geochemical work. The authors wish to thank Roberto De Gennaro for
724 skilled help during EDS microanalyses. Some of the radiocarbon dating in this work was supported by
725 the NERC Radiocarbon Facility NRCF010001 (allocation number 1845.1014). Fieldwork for this work
726 was supported by the UK Natural Environment Research Council (NERC) and Economic and Social
727 Research Council (ESRC) through the Increasing Resilience to Natural Hazards programme [STREVA
728 project, Grant numbers NE/J020001/1. We thank David Pyle and Patrick Bachelery for constructive
729 reviews that improved this manuscript.

730

731 **References**

- 732 Anderson and Yonge 1785 An account of Morne Garou, a Mountain on the island of St Vincent, with
733 a description of the volcano on its summit. *Phil Trans R Soc London* 75:16-31
- 734 Anderson, T., 1908. Report on the Eruption of the La Soufrière in St. Vincent, in 1902, and a Visit to
735 Montagne Pelée in Martinique, Part II, the Change in the Districts and the Subsequent history of
736 the Volcanoes. *Phil. Trans. R. Soc. A* 208, 275–303.
- 737 Anderson, T., Flett, J.S., 1903. Report on the Eruptions of the La Soufrière in St. Vincent, in 1902, and
738 on a Visit to Montagne Pelée in Martinique, Part I. *Phil. Trans. R. Soc. A* 200, 353–553.
- 739 Aspinall, W.P., Sigurdsson, H., Shepherd, J.B., 1973. Eruption of Soufriere Volcano on St Vincent Island.
740 1971-1972. *Science* 181, 117-124.
- 741 Blue Book, 1902. Correspondence relating to the volcanic eruptions in St Vincent and Martinique in
742 May 1902, with map and appendix: Parliamentary Paper by Command, Cd. 1201, HMSO, London.
- 743 Brazier, S., Davis, A.N., Sigurdsson, H., Sparks, R.S.J., 1982. Fallout and deposition of Volcanic ash
744 during the 1979 explosive eruption of the La Soufrière St Vincent. *J. Volcanol. Geotherm. Res.* 14,
745 335-359.
- 746 Briden, J.C., Rex, D.C., Faller, A.M., Tomblin, J.F., 1979. K-Ar geochronology and palaeomagnetism of
747 volcanic rocks in the Lesser Antilles island arc. *Phil. Trans. R. Soc. A* 291, 485-528.
- 748 Bronk Ramsey, C., 2009. Bayesian analysis of radiocarbon dates. *Radiocarbon* 51, 337-360.
- 749 Defoe D (1718) An account of the island of St Vincent in the West Indies and of its entire destruction

750 on 26th March last, with some rational suggestions concerning the causes and manner of it. Mists
751 Weekly J, issues 82, July 5.

752 DeMets, C., Jansma, P.E., Mattioli, G.S., Dixon, T.H., Farina, F., Bilham, R., Calais, E., Mann, P., 2000.
753 GPS geodetic constraints on Caribbean-North America Plate Motion. *Geophys. Res. Lett.* 27, 437-
754 440.

755 Fournier, N., Moreau, M., Robertson, R., 2011. Disappearance of a crater lake: implications for
756 potential explosivity at La Soufrière volcano, St Vincent, Lesser Antilles. *Bull. Volcanol.* 73, 543-555.

757 Graham, A.M., Thirlwall, M.F., 1981. Petrology of the 1979 eruption of La Soufrière Volcano, St.
758 Vincent, Lesser Antilles. *Contrib. Mineral. Petrol.* 76, 336-342.

759 Hay, R.L., 1959. Formation of the Crystal-Rich Glowing Avalanche Deposits of St. Vincent, B.W.I. *J. Geol.*
760 67, 540-562.

761 Heath, E., 1997. Genesis and evolution of calc-alkaline magmas at Soufrière volcano, St. Vincent,
762 Lesser Antilles arc. Unpublished PhD Thesis, University of Lancaster.

763 Heath, E., MacDonald, R., Belkin, H., Hawkesworth, C., Sigurdsson, H., 1998. Magmagenesis at La
764 Soufrière Volcano, St Vincent, Lesser Antilles Arc. *J. Petrol.* 39, 1721-1764.

765 Hovey, E.O., 1903. Martinique and St. Vincent; a Preliminary Report upon the Eruptions of 1902. *Bull.*
766 *Am. Mus. Nat. Hist.* 16, 333–372.

767 Irvine, T., Baragar, W., 1971. A guide to the chemical classification of the common volcanic rocks. *Can.*
768 *J. Earth Sci.* 8, 523-548.

769 Lamb, O., Varley, N.R., Mather, T.A., Pyle, D.M., Smith, P.J., Liu, E.J., 2014. Multiple timescales of
770 cyclical behavior observed at two dome-forming eruptions. *J. Volcanol. Geotherm. Res.* 284, 106-
771 121.

772 Le Friant, A., Boudon, G., Arnulf, A., Robertson, R.E.A., 2009. Debris avalanche deposits offshore St.
773 Vincent (West Indies): Impact of flank-collapse events on the morphological evolution of the island.
774 *J. Volcanol. Geotherm. Res.* 179, 1-10.

775 Le Maitre, R.W., 2002. *Igneous Rocks: A Classification and Glossary of Terms. Recommendations of*
776 *the International Union of Geological Sciences Subcommittee on the Systematics of Igneous*
777 *Rocks.* Cambridge University Press, Cambridge, UK, 256 pp.

778 Luhr, J.F., Carmichael, I.S.E., 1990. Petrological monitoring of cyclical eruptive activity at Volcán
779 Colima, Mexico. *J. Volcanol. Geotherm. Res.* 42, 235-260.

780 McBirney, H., Williams, A.R., 1979. *Volcanology*. Freeman, Cooper & Co, 400 pp.

781 Macdonald, R., Hawkesworth, C., Heath, E., 2000. The Lesser Antilles volcanic chain: a study in arc
782 magmatism. *Earth-Sci. Rev.* 49, 1-76.

783 Melekhova, E., Blundy, J., Robertson, R., Humphreys, M.C.S., 2015. Experimental evidence for
784 polybaric differentiation of primitive arc basalt beneath St. Vincent, Lesser Antilles. *J. Petrol.* 56,
785 161-192.

786 Morimoto, N., 1988. Nomenclature of pyroxenes. *Mineral. Petrol.* 39, 55-76.

787 Odbert, H.M., Stewart, R.C., Wadge, G., 2014. Chapter 2 - Cyclic phenomena at the La Soufrière Hills
788 Volcano, Montserrat. In: Wadge, G., Robertson, R.E.A., Voight, B. (eds.), *The Eruption of Soufrière
789 Hills Volcano, Montserrat from 2000 to 2010*. Geological Society, London, *Memoirs* 39, 41-60. doi:
790 10.1144/M39.2

791 Pichavant, M., Macdonald, R., 2007. Crystallization of primitive basaltic magmas at crustal pressures
792 and genesis of the calc-alkaline igneous suite: experimental evidence from St. Vincent, Lesser
793 Antilles arc. *Contrib. Mineral. Petrol.* 154, 535-558.

794 Pichavant, M., Mysen, B.O., Macdonald, R., 2002. Source and H₂O content of high-MgO magmas in
795 island arc settings: an experimental study of primitive calc-alkaline basalt from St. Vincent, Lesser
796 Antilles arc. *Geochim. Cosmochim. Acta* 66, 2193-2209.

797 Pindell, J.L., Cande, S.C., Pitman III, W.C., Rowley, D.B., Dewey, J.F., LaBrecque, J., Haxby, W., 1988. A
798 plate-kinematic framework for models of Caribbean evolution. *Tectonophysics* 155, 121-138.

799 Pyle, D.M., Barclay, J., Armijos, M.T., 2018. The 1902–3 eruptions of the Soufrière, St Vincent: Impacts,
800 relief and response. *J. Volcanol. Geotherm. Res.* 356, 183-199.

801 Robertson, R.E.A., 1992. Volcanic hazard and risk assessment of the La Soufrière volcano, St. Vincent,
802 West Indies. Unpublished MPhil thesis.

803 Robertson, R.E.A., 2005 St Vincent. In: Lindsay, J., Robertson, R., Shepherd, J., Ali, S. (eds.), *Volcanic
804 Hazard Atlas of the Lesser Antilles*.

805 Roobol, M.J., Smith, A.L., 1975. A comparison of the recent eruptions of Mt. Pelée, Martinique and La
806 Soufrière, St. Vincent. *Bull. Volcanol.* 39, 214-240.

807 Rowley, K., 1978a. Stratigraphy and geochemistry of the Soufriere volcano, St. Vincent WI.
808 Unpublished PhD thesis.

809 Rowley, K., 1978b. Late Pleistocene pyroclastic deposits of Soufrière Volcano, St. Vincent, West Indies.
810 Geol. Soc. Am. Bull. 6, 825-835.

811 Shepherd, C., 1831. An historical account of the island of Saint Vincent. Nicol, London, 216 pp.

812 Shepherd, J.B., Sigurdsson, H., 1982. Mechanism of the 1979 explosive eruption of soufriere volcano,
813 St. Vincent. J. Volcanol. Geotherm. Res. 13, 119-130.

814 Shepherd, J.B., Aspinall, W.P., Rowley, K.C., Pereira, J., Sigurdsson, H., Fiske, R.S., Tomblin, J.F., 1979.
815 The eruption of Soufriere volcano, St. Vincent, April-June 1979. Nature 282, 24-28.

816 Smith, S.D., 2011, Volcanic hazard in a slave society: the 1812 eruption of Mount La Soufrière in St
817 Vincent. J. Hist. Geogr. 37, 55-67.

818 Smith, T.E., Thirlwall, M.F., Macpherson, C., 1996. Trace element and isotope geochemistry of the
819 volcanic rocks of Bequia, Grenadine Islands, Lesser Antilles Arc: a study of subduction enrichment
820 and intra-crustal contamination. J. Petrol. 37, 117-143.

821 Sparks, R.S.J., Aspinall, W.P., 2004. Volcanic activity: frontiers and challenges in forecasting, prediction
822 and risk assessment. In: Sparks, R.S.J., Hawkesworth, C.J. (eds.), The state of the planet: frontiers
823 and challenges in geophysics. Washington, DC: American Geophysical Union, pp. 359-373.
824 doi:10.1029/150GM28

825 Stuiver, M., Reimer, P.J., and Reimer, R.W., 2018. CALIB 7.1 [WWW program] at <http://calib.org>,
826 accessed 2018-7-9

827 Tollan, P.M.E., Bindeman, I., Blundy, J.D., 2012. Cumulate xenoliths from St. Vincent, Lesser Antilles
828 Island Arc: a window into upper crustal differentiation of mantle-derived basalts. Contrib. Mineral.
829 Petrol. 163, 189-208.

830

831

832

833 **Electronic Supplementary Material 1** Representative whole-rock, mineral chemistry and glass
834 composition data for the analysed scoria samples from the 1440 CE, 1580 CE, 1718-1812 and 1902-
835 03 eruptions of the La Soufrière volcano.

836 **Table SM1** Representative major element concentrations (wt.%) and calculated structural formulae
837 (apfu, atoms per formula unit, on 6 oxygens and 4 cations) for clinopyroxene (cpx) and
838 orthopyroxene (opx) crystals from the analysed scoria samples from the 1440 CE, 1580 CE, 1718-

839 1812 and 1902-03 eruptions of the La Soufrière volcano.

840 * = mafic-rich scoria

841 bdl = below detection limits

842 Mg# = $Mg/(Mg+Fe^{2+})$; En = enstatite mol.%; Wo = wollastonite mol.%; Fs = ferrosilite mol.%

843 cpx-anh = anhedral cpx; mpc = microphenocryst

844

845 **Table SM2** Representative major element concentrations (wt.%) and calculated structural formulae
846 (apfu, atoms per formula unit, on 8 oxygens and 5 cations) for plagioclase crystals (pl) from the
847 analysed scoria samples from the 1440 CE, 1580 CE, 1718-1812 and 1902-03 eruptions of the La
848 Soufrière volcano.

849 * = mafic-rich scoria

850 bdl = below detection limits

851 Ab = albite mol.%; Or = orthoclase mol.%; An = anorthite mol.%

852 pl-anh = anhedral pl; mpc = microphenocryst

853

854 **Table SM3** Representative major element concentrations (wt.%) and calculated structural formulae
855 (apfu, atoms per formula unit) for olivine crystals (ol, on 4 oxygens and 3 cations) from the analysed
856 scoria samples from the 1440 CE, 1718-1812 and 1902-03 eruptions of the La Soufrière volcano.

857 * = mafic-rich scoria

858 bdl = below detection limits

859 Mg# = $Mg/(Mg+Fe^{2+})$; Fo = forsterite mol.%; Fa = fayalite mol.%; Teph = tephroite mol.%

860 ol-anh = anhedral ol; mpc = microphenocryst

861

862 **Table SM4** Representative major element concentrations (wt.%) and calculated structural formulae
863 (apfu, atoms per formula unit) for Ti-magnetite crystals (mt, on 4 oxygens and 3 cations) from the
864 analysed scoria samples from the 1440 CE, 1580 CE, 1718-1812 and 1902-03 eruptions of the La
865 Soufrière volcano.

866 * = mafic-rich scoria

867 bdl = below detection limits

868 Ulvöspinel mol% (Usp%), and FeO and Fe₂O₃ were calculated following Carmichael (1967)

869 Mg# = $Mg/(Mg+Fe^{2+})$; Cr# = $Cr/(Cr+Al)$

870 mpc = microphenocryst; in ol = inclusion in olivine; in cpx = inclusion in clinopyroxene; in opx =
871 inclusion in orthopyroxene

872

873 **Table SM5** Representative major element concentrations (wt.%) for groundmass glass from the
874 analysed scoria samples from the 1440 CE, 1580 CE, 1718-1812 and 1902-03 eruptions of the La
875 Soufrière volcano.

876 * = mafic-rich scoria

877 bdl = below detection limits

878 $Mg\# = Mg/(Mg+Fe^{2+})$

879 gm = groundmass; in ol = inclusion in olivine; in cpx = inclusion in clinopyroxene; in pl = inclusion in
880 plagioclase; in opx = inclusion in orthopyroxene

881

882 **Table SM6** Major- and trace element concentrations (respectively in wt.% recalculated to 100% on a
883 water-free basis, and in ppm) for the analysed scoria samples from the 1440 CE, 1580 CE, 1718-1812
884 and 1902-03 eruptions of the La Soufrière volcano.

885 * = mafic-rich scoria

886 bdl = below detection limits

887 $Mg\# = \text{molar } Mg/(Mg+Mn+Fe^{2+})$

888

889 Figure SM1